Cancer Management and Research

Dovepress

open access to scientific and medical research

Open Access Full Text Article

ORIGINAL RESEARCH

miR-31-5p Regulates *14-3-3 ε* to Inhibit Prostate Cancer 22RV1 Cell Survival and Proliferation via PI3K/AKT/Bcl-2 Signaling Pathway

This article was published in the following Dove Press journal:
Cancer Management and Research

Jiafu Zhao[1–3]
Houqiang Xu[1–3]
Zhiqiang Duan[2,3]
Xiang Chen[2,3]
Zheng Ao[2,3]
Yinglian Chen[2,3]
Yong Ruan[2,3]
Mengmeng Ni[2,3]

[1]College of Life Science, Guizhou University, Guiyang 550025, People's Republic of China; [2]Key Laboratory of Animal Genetics, Breeding and Reproduction in the Plateau Mountainous Region, Ministry of Education, Guizhou University, Guiyang 550025, People's Republic of China; [3]College of Animal Science, Guizhou University, Guiyang 550025, People's Republic of China

Introduction: Prostate cancer (PCa) is one of the most common malignancies, and almost all patients with advanced PCa will develop castration-resistant prostate cancer (CRPC) after receiving endocrine therapy. Effective treatment for patients with CRPC has not been established. Novel approaches are needed to identify therapeutic targets for CRPC.

Purpose: Recent research studies have found that members of the 14-3-3 family play an important role in the development and progression of PCa. Previous results have shown that *14-3-3 ε* is significantly upregulated in several cancers. This study aimed to identify novel miRNAs that regulate 14-3-3 ε expression and therapeutic targets for CRPC.

Methods: In this study, we used computation and experimental approaches for the prediction and verification of the miRNAs targeting 14-3-3 ε, and investigated the potential roles of 14-3-3 ε in the survival and proliferation of 22RV1 cells.

Results: We confirm that mir-31-5p is downregulated in 22RV1 cells and acts as a tumor suppressor by regulating *14-3-3 ε*. Ectopic expression of miR-31-5p or *14-3-3 ε* interference significantly inhibits cell proliferation, invasion, and migration in 22RV1 cells, as well as promotes cell apoptosis via the PI3K/AKT/Bcl-2 signaling pathway. Moreover, *14-3-3 ε* is required for the miR-31-5p-mediated upregulation of the PI3K/AKT/Bcl-2 signaling pathway.

Conclusion: Our findings provide information on the underlying mechanisms of miR-31-5p/*14-3-3 ε* in 22RV1 cell proliferation and apoptosis through the PI3K/AKT/Bcl-2 signaling pathway. These results suggest that miR-31-5p and 14-3-3 ε may potentially be utilized as novel prognostic markers and therapeutic targets for PCa treatment.

Keywords: prostate cancer, miR-31-5p, *14-3-3 ε*, PI3K/AKT/Bcl-2 pathway, cell proliferation, cell apoptosis

Introduction

Prostate cancer (PCa) is one of the most common malignancies and the second most prevalent cancers in men worldwide.[1] Approximately 5% of diagnosed patients develop locally advanced PCa, while 10% evolve to distant metastasis.[2] Early-stage PCa can be treated with androgen deprivation therapy (ADT). However, almost all patients with advanced PCa will develop castration-resistant prostate cancer (CRPC) after receiving endocrine therapy.[3] CRPC is also referred to as hormone-refractory or androgen-independent prostate cancer (AIPC).[4] AIPC is an incurable PCa that bypasses the normal pathway of androgen-dependent growth and survival. Generally, treatment with androgen ablation eventually leads to AIPC.[5] Although

Correspondence: Houqiang Xu
College of Life Science, Guizhou University, No. 197, Huashi Road, Huaxi District, Guiyang City, Guizhou Province, People's Republic of China
Tel +86 13765056884
Fax +86 851 88298005
Email gzdxxhq@163.com

submit your manuscript | www.dovepress.com
DovePress
http://doi.org/10.2147/CMAR.S247780

the androgen receptor (AR) is an effective way to treat metastatic castrate-resistant prostate cancer (mCRPC),[6] 29,430 people died of PCa in the USA in 2018.[7] AR is a ligand-activated transcription factor that regulates numerous target genes, including prostate-specific antigen (PSA).[8] Recently, one study showed that members of the 14-3-3 family play an important role in the development and progression of PCa, which can regulate the transcription of PSA through the AR.[8] This family may be used as a novel target for the diagnosis and treatment of PCa.[9]

14-3-3 Proteins are a family of conserved regulatory molecules that are expressed in eukaryotic cells.[10] 14-3-3 Proteins regulate intracellular signaling pathways through the phosphorylation of serine/threonine motifs of target proteins that are related to signal transduction, protein trafficking, cell cycle, and apoptosis.[11] In mammals, 14-3-3 proteins consist of nine isoforms, including two phosphorylated forms (α and δ) that are encoded by seven genes (β, γ, ε, ζ, η, σ, and τ).[12] 14-3-3 ε, which is encoded by the *YWHAE* gene on chromosome 17,[13] is a major regulator of apoptotic pathways critical to cell survival and plays a key role in the development of hepatocellular carcinoma,[14] lung cancer,[15] breast cancer,[16] vulvar squamous cell carcinoma,[17] follicular and papillary thyroid tumors,[18] meningioma,[19] HCC,[20] and gastric cancer.[21] KO and his colleagues analyzed the pathological specimens of 114 patients with liver cancer and found that the high expression of 14-3-3ε protein was associated with the migration of liver cancer.[20] Liou et al found that the stable expression of 14-3-3ε in HT-29 cells prevented apoptosis, as well as elucidated a novel mechanism by which nonsteroidal anti-inflammatory drugs could induce apoptosis in colorectal cancer cells through the PPAR/14-3-3ε pathway.[22] Liang et al found that the expression of 14-3-3ε was upregulated by 1.44-fold in renal cancer tissues, and in vitro experiments confirmed that 14-3-3ε could promote the abnormal proliferation of renal tumor cells.[23] Li et al used proteomics to compare the protein expression of different metastatic breast cancer cell lines and found that the expression level of 14-3-3ε in lowly metastatic tumor cells was higher than that in highly metastatic cell lines.[16] Recently, Alex and colleagues[9] have suggested that 14-3-3ε and other family members play an important role in the development and progression of PCa, and thus can be potentially used as drug targets in the treatment of PCa. In addition, 14-3-3ε may serve as a novel prognostic biomarker or therapeutic target for HCC,[14] breast cancer,[12] and HIV neurocognitive impairments.[24] Although previous studies have indicated that 14-3-3ε can be used as drug targets in the treatment of PCa, its specific mechanism remains unclear. Currently, chemotherapeutic drugs that target 14-3-3ε in PCa mainly include docetaxel and a non-peptidic small-molecule inhibitor of SFN known as BV02.[9] However, due to the harmful side effects of chemotherapeutic drugs, there is an urgent need to identify safer therapies for PCa.

MicroRNAs (miRNAs) are a class of small non-coding RNAs with a length of 18–26 nucleotides (nt) that can regulate gene expression through post-transcriptional repression or mRNA degradation. Several studies have confirmed that multiple miRNAs are involved in the proliferation, progression, and metastasis of various cancers.[25–27] Therefore, screening miRNAs involved in regulating *14-3-3 ε* expression and exploring the molecular mechanism underlying miRNA-mediated proliferation and apoptosis of PCa cells are of great significance for the early diagnosis and targeted drug therapy of PCa.

In this study, we used computation and experimental approaches for the prediction and verification of miRNA targeting *14-3-3 ε* and investigated the potential roles of 14-3-3 ε in the survival and proliferation of PCa cells. Online database analysis identified five potential miRNAs that target *14-3-3 ε*. We demonstrated that miR-31-5p negatively regulates the expression of *14-3-3 ε* via its 3′UTR. In addition, our studies revealed that the upregulation of miR-31-5p inhibits PCa cell proliferation, invasion, and migration, as well as increased the activity of the PI3K/AKT/Bcl-2 signaling pathway. Moreover, 14-3-3 ε is required for the miR-31-5p-mediated upregulation of the PI3K/AKT/Bcl-2 signaling pathway. In conclusion, our results suggest that miR-31-5p might inhibit PCa cell proliferation and promote cell apoptosis by targeting *14-3-3 ε* via the PI3K/AKT/Bcl-2 signaling pathway, which provides evidence that miR-31-5p and *14-3-3 ε* may be potentially utilized as prognostic biomarkers and therapeutic targets for PCa treatment.

Materials and Methods

miRNA Screening

According to the recognition mechanism of miRNAs and mRNAs, TargetScan (www.targetscan.org; version 7.2), miRSystem (mirsystem.cgm.ntu.edu.tw; version 21), miRanda (www.microrna.org; version 2010), and PicTar (www.pictar.org; version 2007) were used to predict miRNAs that potentially bind to the 3′-UTR of *14-3-3ε*.

The five miRNAs (has-miR-155-5p, has-miR-31-5p, has-miR-29a-3p, has-miR-29b-3p, and has-miR-29c-3p) with high screening scores were selected as candidates by logical estimates.

Cells and Antibodies

The human normal prostate stromal immortalized cell line WPMY-1 and three human PCa cell lines PC3, 22RV1, and LNCaP were purchased from Shanghai Zhong Qiao Xin Zhou Biotechnology Co., Ltd. LNCaP cells were cultured in RPMI-1640 medium (Gibco-BRL, Invitrogen; Paisley, UK), supplemented with 10% FBS, 1% penicillin-streptomycin, 2% HEPES, 1% Glutamax (Invitrogen, 35050, USA), and 1% sodium pyruvate (Invitrogen, 11360070, USA). WPMY-1, PC3, and 22RV1 cells were cultured in DMEM high-glucose medium/F12 (1:1) medium, RPMI-1640 medium (Gibco), and EMEM medium (Zhong Qiao Xin Zhou, Shanghai, China), respectively, and supplemented with 10% fetal bovine serum (Gibco) and 1% penicillin-streptomycin. All cells were maintained at 37°C in 5% CO_2 atmosphere. The 22RV1 cell line was derived from a xenograft human PCa epithelial cell line, is androgen-independent, and can respond to androgen after endocrine therapy.[28,29] In addition, this cell line expresses androgen receptor (AR). Based on these properties, we used 22RV1 cells in the cell phenotype validation test. Anti-GAPDH (Cat. No. 60004-1-Ig), anti-14-3-3ε (Cat. No. 66946-1-Ig), anti-PI3K (Cat. No. 67071-1-Ig), anti-AKT (Cat. No. 60203-1-Ig) mouse monoclonal antibodies, anti-BAD (Cat. No. 10435-1-AP), and anti-BAX (Cat. No. 50599-2-Ig) rabbit polyclonal antibodies were purchased from Proteintech (Proteintech, Wuhan, China). Anti-caspase-3 (#9668), phosphor-PI3K (Ser249) (#13857), and phosphor-AKT (Ser473) (#4060) mouse monoclonal antibodies were purchased from Cell Signaling Technology (Cell Signaling Technology, Carlsbad, CA, USA). Rabbit monoclonal antibodies against Bcl-2 (ab182858) and caspase-9 (ab202068) were purchased from Abcam (Abcam, USA).

Plasmid Construction

All enzymes used for cloning procedures were purchased from TakaRa Company. The miR-31-5p binding site in the 3′-UTR of *14-3-3ε* was identified by bioinformatics analysis using microRNA.org (http://www.microrna.org/microrna/home.do). The wild-type fragment 3′-UTR of *14-3-3ε* that contained potential miR-31-5p binding sites at position 608–614 was amplified from the cDNA derived from 22RV1 cells using the following primers: 5′-CCCT CGAGACATTTGAAAGCCATTAGACT-3′ (forward) and 5′-GCGTCG ACAGGTTGAGCGAGCGAAG-3′ (reverse), and then subcloned into pmirGLO to create pGL-WT-*14-3-3 ε*/3′UTR. The mutant-type fragment 3′-UTR of *14-3-3ε* was directly synthesized by Shanghai Qingke Biotechnology Co., Ltd. (Shanghai, China) and then subcloned into pmirGLO to create pGL-MT-*14-3-3ε*/3′UTR. *14-3-3ε* cDNAs were obtained by RT-PCR using 22RV1 cells and subcloned into pCI-neo (Clontech/Takara) plasmids. All recombinant plasmids were confirmed by PCR, restriction digestion, and DNA sequencing. For *14-3-3ε* silencing, a pool of four different double-stranded siRNAs (Table 1) targeting *14-3-3 ε* or scrambled control siRNAs were synthesized by Shanghai Qingke Biotechnology Co., Ltd. (Shanghai, China). All siRNA experiments were performed at least three times.

Table 1 The Information of 14-3-3 ε siRNAs in This Paper

siRNA Name	Sequences of siRNA (5′→3′)	
h-14-3-3 ε-siRNA-1	Sense Antisense	GCUGAGCGAUACGACGAAATT UUUCGUCGUAUCGCUCAGCTT
h-14-3-3 ε-siRNA-2	Sense Antisense	GCUGCUAGUGAUAUUGCAATT UUGCAAUAUCACUAGCAGCTT
h-14-3-3 ε-siRNA-3	Sense Antisense	CAAAAGCAGCUUUUGAUGATT UCAUCAAAAGCUGCUUUUGTT
h-14-3-3 ε-siRNA-4	Sense Antisense	GCAGUUGUUACGUGAUAAUTT AUUAUCACGUAACAACUGCTT
Negative control	Sense Antisense	UUCUCCGAACGUGUCACGUdTdT ACGUGACACGUUCGGAGAAdTdT

Cell Transfection and Western Blotting

The constructed plasmids, miRNA mimics (has-miR-31-5p, negative control; GenePharma Co., Ltd., Shanghai, China), miRNA inhibitors (has-miR-31-5p inhibitor, microRNA inhibitor N.C.; GenePharma Co., Ltd., Shanghai, China), pCI- neo-14-3-3 ε, pCI-neo, siRNAs (si-RNA1, si-RNA2, si-RNA3, and si-RNA4), and siRNA negative control were transfected into 22RV1 cells using FuGENE® HD Transfection Reagent (Promega, USA) after cells were grown to 70–80% confluency, with 2500 ng of plasmid or 50 nM miRNA mimics used per well in 6-well plates. The 22RV1 cells were harvested at 36 h post-transfection (hpt) to extract cellular proteins. The lysates (50 μg) were resolved by SDS-PAGE and transferred onto PVDF membranes.

Antibodies against GAPDH, BAD, Bcl-2, caspase-9, caspase-3, and 14-3-3 ε were used to detect the effect of overexpressing or inhibiting miR-31-5p or 14-3-3 ε on the expression of proteins mentioned above in 22RV1 cells.

Quantitative Real-Time PCR (qRT-PCR)

Total RNA was extracted from 22RV1 cells using the TRIzol reagent (Invitrogen, Carlsbad, CA, USA) and reversely transcribed into cDNA using ThermoFisher Scientific Revert Aid First Strand cDNA Synthesis Kit. qRT-PCR was performed on a BioRad C1000 detection system (BioRad) using a QuntiFast® SYBR® Green PCR kit (QIAGEN) following the manufacturer's instructions. The RNA expression levels of *14-3-3 ε* or the five miRNAs were calculated relative to the expression of GAPDH or U6 small nuclear RNA. Reverse and qRT-PCR primers that were designed by software Primer 5.0 and Oligo 7.0 are shown in Tables 2 and 3. The data were analyzed using the $2^{-\Delta\Delta CT}$ method.

Table 3 qRT-PCR Primers Used in This Study

Gene Name	Sequence (5′→3′)	Amplified Length (bp)
miR-155-5p/Q-F	CGCGCTTAATGCTAATCGTGA	82
miR-31-5p/Q-F	CAAGAGGCAAGATGCTGGCA	79
miR-29a-3p/Q-F	TCCCGTAGCACCATCTGAAAT	80
miR-29b-3p/Q-F	TCGGCTAGCACCATTTGAAAT	81
miR-29c-3p/Q-F	GGCGGTAGCACCATTTGAAAT	80
miR-Universal/Q-R	CAAAGCAGGGTCCGAGGTATC	
14-3-3 ε/Q-F	TAAAATGAAAGGGGACTACCACA	161
14-3-3 ε/Q-R	TGAGAGCAAGACCTAAGCGAATA	
GAPDH-F	AAATCCCATCACCATCT	116
GAPDH-R	CCCCAGCCTTCTCCAT	
U6-F	CTCGCTTCGGCAGCACA	93
U6-R	AACGCTTCACGAATTTGCGT	

Abbreviations: miR, microRNA; F, forward; R, reverse; Q-F, quantitative polymerase chain reaction forward primer; Q-R, quantitative polymerase chain reaction forward primer.

Luciferase Reporter Assay

22RV1 cells were co-transfected with miRNA or negative control, together with 100 ng of pGL3-WT-14-3-3ε/3′ UTR or pGL3-MT-14-3-3ε/3′ UTR and 100 ng control vector pGL3 (Promega, Madison, WI, USA) using FuGENE® HD Transfection Reagent according to the manufacturer's protocol. The cells were harvested at 24 hpt and subjected to the Dual-Glo® Luciferase Assay System (Promega, USA). The cells were seeded into 96-well plates with each well containing 75 μL of Dual-Glo® Luciferase Reagent, mixed, and incubated for 20 min. Firefly luminescence activity was later measured using a multi-mode microplate reader (BioTek, Winooski, VT, USA). Later, an equal volume of Dual-Glo® Stop & Glo® Reagent was added to each well, and then *Renilla* luciferase activity was measured using the same method earlier described. The results were expressed as the ratio of firefly to *Renilla* luciferase activity for each well.

CCK-8 Assay

An Enhanced Cell Counting Kit-8 (CCK-8) (Saint-Bio, Shanghai, China) was used to determine cell viability. Briefly, cells were transfected with miR-31-5p and negative control using FuGENE® HD transfection reagent. The 22RV1 cells were seeded into 96-well plates at a density of 1×10^5 cells/well and incubated for 12 h. Then, cell viability was measured at 0, 24, 48, and 72 h after transfection. At each time point, 100 μL culture medium was harvested and then mixed with 10 μL of the CCK-8 reagent. The plates were incubated at 37°C for 3 h. The absorbance was measured at a wavelength of 490 nm using a multi-mode microplate reader (BioTek). All experiments were performed in sextuplicate.

Table 2 MicroRNA Reverse Primers Were Used in This Study

Gene Name	Sequence (5′→3′)
Stem loop sequence	GGTCGTATGCAAAGCAGGGTCCGAGGTATCCATCGCACGCATCGCACTGCATACGACC
RT-miR-155-5p	GGTCGTATGCAAAGCAGGGTCCGAGGTATCCATCGCACGCATCGCACTGCATACGACC**AACCCCTA**
RT-miR-31-5p	GGTCGTATGCAAAGCAGGGTCCGAGGTATCCATCGCACGCATCGCACTGCATACGACC**AGCTATGC**
RT-miR-29a-3p	GGTCGTATGCAAAGCAGGGTCCGAGGTATCCATCGCACGCATCGCACTGCATACGACC**TAACCGAT**
RT-miR-29b-3p	GGTCGTATGCAAAGCAGGGTCCGAGGTATCCATCGCACGCATCGCACTGCATACGACC**AACACTGA**
RT-miR-29c-3p	GGTCGTATGCAAAGCAGGGTCCGAGGTATCCATCGCACGCATCGCACTGCATACGACC**TAACCGAT**
R-U6	AACGCTTCACGAATTTGCGT

Note: Underlined sequences indicate miRNA interaction sites in the 3′-untranslated region.
Abbreviations: RT, reverse transcription; R, reverse; miR, microRNA.

Transwell® Assay

Transwell® assays were performed to measure the invasion ability of 22RV1 cells. For the cell invasion assay, 100 μL of diluted Matrigel® was added to the bottom center of the chamber and incubated at 37°C for 3 h. Then, 2×10^5 cells were added into the Transwell® inserts of 8 mm in size in 24-well plates (Corning Inc., Corning, NY, USA). Then, the upper Transwell® chambers were mixed with 150 μL serum-free medium, and the bottom chamber contained medium with 20% FBS as chemoattractant. After 24 h incubation at 37°C, the inserts were washed thrice with phosphate-buffered saline (PBS), fixed with 800 μL methanol for 30 min, and then stained with Giemsa for 30 min at room temperature. Cell invasion was quantified by counting the number of cells in five random fields. The data were expressed as the average number of cells per insert.

Scratch Wound Healing Assays

22RV1 cells were plated into 6-well plates with complete medium and incubated overnight until 70% confluency. Cells were transfected with the appropriate plasmid or microRNA. A 100-μL sterile pipette tip was used to generate a wound in the cell layer at 6 hpt. The plates were then washed with PBS to remove the scraped cells. Cell migration distance across the same scraped area was captured at 0 h and 24 h. Each test was conducted independently in triplicate.

Apoptosis Assay

Apoptosis was detected using an Annexin V-FITC apoptosis detection kit containing Annexin V-FITC and propidium iodide (PI). The 22RV1 cells were seeded into six-well plates at a density of 3×10^5 per well and maintained in complete medium for 12 h until 70% confluency. The cells were then transfected with miR-31-5p, pCI-14-3-3ε, miR-31-5p + pCI-14-3-3ε, or their respective control. At 48 hpt, the cells were washed once with PBS, harvested, and centrifuged at 1000g for 5 min. Then, the cells were incubated in 195 μL of Annexin V-FITC binding buffer with 5 μL of Annexin V-FITC and 10 μL of PI for 20 min at room temperature in the dark. Annexin staining was measured by fluorescence microscopy (Nikon, Japan).

Statistical Analysis

The results of this study were expressed as the mean ± SD of at least three independent experiments. *T*-test and multiple comparisons with LSD were performed wherever appropriate using GraphPad Prism software ver. 6.0; differences with P values <0.01 were considered extremely significant, whereas those with P values <0.05 were considered significant. "*" represents $P < 0.05$ and "**" represents $P < 0.01$ in the *t*-test. However, when multiple comparisons were performed, different capital letters indicate extremely significant difference ($P < 0.01$), different lowercase letters indicate significant difference ($P < 0.05$), and the same letter indicates no significant difference ($P > 0.05$).

Results

Screening and Identification of miRNAs Targeting 14-3-3 ε

Bioinformatics analysis using TargetScan, miRanda, and DIANA identified five candidate miRNAs, including miR-155-5p, miR-31-5p, miR-29a-3p, miR-29b-3p, and miR-29c-3p. Then, the transfection efficiency of miRNAs was assessed at 24 and 48 hpt in the treatment group, negative control, and blank group. The results showed that five candidate miRNAs reached an extremely significant difference ($P < 0.01$) both at 24 hpt and 48 hpt (Figure 1A). To screen the more effective miRNA that regulates the expression of *14-3-3 ε* genes, the inhibition efficiency of the five miRNAs on the *14-3-3 ε* genes were analyzed by qRT-PCR and dual luciferase activity experiments at 24 hpt (Figure 1B). The results demonstrated that miR-31-5p and miR-29b-3p significantly decreased *14-3-3ε* mRNA expression ($P < 0.01$), whereas miR-29a-3p and miR-29c-3p significantly increased *14-3-3ε* mRNA expression in PC3 cells ($P < 0.01$). However, miR-155-5p did not significantly increase *14-3-3ε* mRNA levels ($P > 0.05$) compared with the negative control (NC) group. Dual luciferase activity experiments showed that miR-155-5p, miR-31-5p, and miR-29b-3p could significantly regulate the relative luciferase activity of *14-3-3ε* ($P < 0.01$), whereas miR-29a-3p and miR-29c-3p had no significant difference ($P > 0.05$) (Figure 1C). Studies on the expression of miR-155-5p, miR-31-5p, and miR-29b-3p in PC3, LNCaP, 22RV1, and WPMY-1 cells showed that the expression levels of miR-155-5p, miR-31-5p, and miR-29b-3p in PCa cells decreased compared to the WPMY-1 cells. The five miRNAs, except for miR-31-5p, did not reach significant levels in PC3 cells ($P > 0.05$), whereas the others reached extremely significant levels ($P < 0.01$) compared to WPMY-1 (Figure 1D). In addition, cell viability experiments showed that three miRNAs (miR-155-5p, miR-31-5p, and miR-29b-3p) significantly inhibited the proliferation of 22RV1 cells at 72 hpt ($P < 0.01$) (Figure 1E). Based on the

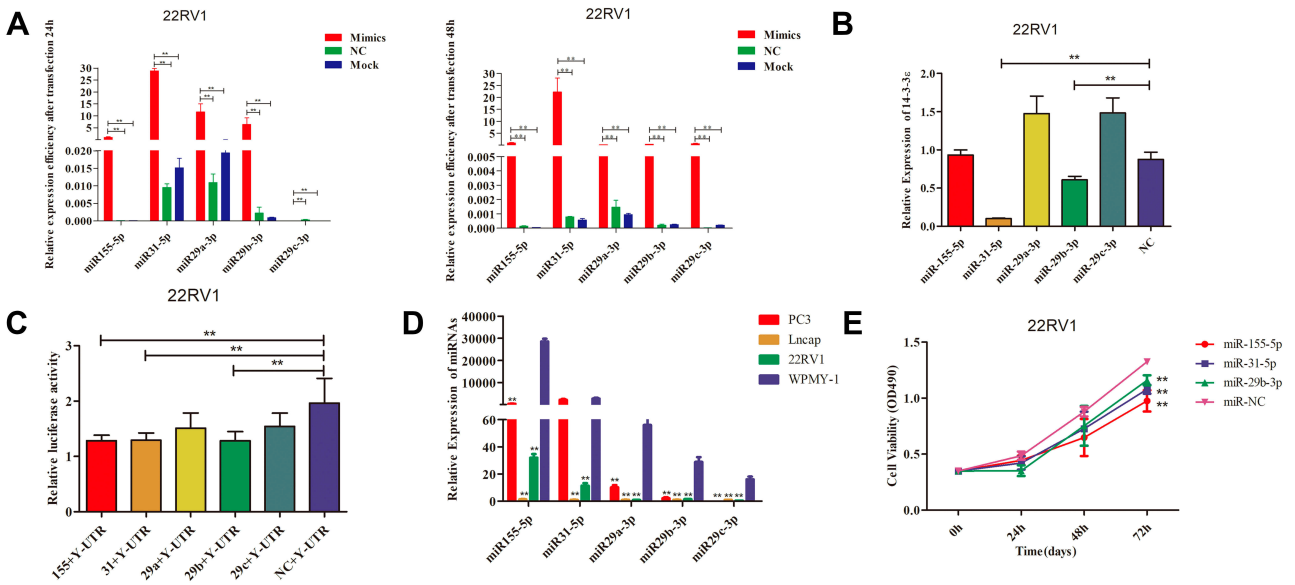

Figure 1 Screening and identification of miRNAs targeting*14-3-3 ε*.(**A**) The transfection efficiency of miR-155-5p, miR-31-5p, miR-29a-3p, miR-29b-3p, and miR-29c-3p in 22RV1 cells were detected by qRT-PCR at 24 and 48 hpt. (**B**) The effect of miR-155-5p, miR-31-5p, miR-29a 3p, miR-29b-3p, and miR-29c-3p on regulating the expression of 14-3-3 ε in 22RV-1 cells. (**C**) After transfection, luciferase activity was assessed using a dual-luciferase reporter assay system. Each value was evaluated based on the relative luciferase activity of firefly to Renilla. (**D**) Expression levels of miR-155-5p, miR-31-5p, miR-29a-3p, miR-29b-3p, and miR-29c-3p in three PCa cell lines (PC3, LNCaP, and 22RV-1) and normal PCa cells (WPMY-1) were determined using qRT-PCR. WPMY-1 was used as the internal control. (**E**) Effect of miR-155-5p, miR-31-5p, and miR-29b-3p overexpression on 22RV-1 cell viability. The data are presented as the mean ± standard deviation of three independent experiments. Statistical significance was determined using the Student's *t*-test. $^{**}P < 0.01$ vs control group.

above experimental results, we found that mir-31-5p had the best inhibitory effect on *14-3-3 ε*, and thus was employed in the subsequent experimental studies.

To investigate whether miR-31-5p could directly bind *14-3-3ε*, miR-31-5p mimics or miR-31-5p inhibitor was used to induce ectopic or inhibit miR-31-5p expression. To confirm the interaction between miR-31-5p and *14-3-3 ε*, pGL-WT-14-3-3 ε/3′UTR and pGL-MT-14-3-3 ε/3′UTR vector were constructed (Figure 2A) and co-transfected with miR-31-5p mimics or miR-31-5p inhibitor into 22RV1 cells. The results of dual luciferase reporter gene assay showed that the luciferase activity of 22RV1 cells transfected with WT-14-3-3 ε/3′UTR +miR-31-5p group was significantly suppressed in comparison to WT-14-3-3 ε/3′UTR +NC mimics, WT-14-3-3 ε/3′UTR +miR-31-5p inhibitor and WT-14-3-3 ε/3′UTR +NC inhibitor groups ($P < 0.01$). However, the luciferase activity in the MT-14-3-3 ε/3′UTR +NC mimic group did not significantly change ($P > 0.05$) (Figure 2B). These results indicate that *14-3-3 ε* mRNA 3′UTR is a specific functional target of miR-31-5p in 22RV1 cells.

14-3-3 ε and miR-31-5p are Differentially Expressed in PCa Cell Lines

The expression patterns of *14-3-3ε* and miR-31-5p in PCa cell lines were then investigated. To investigate the expression of *14-3-3ε* in prostate adenocarcinoma (PRAD), the

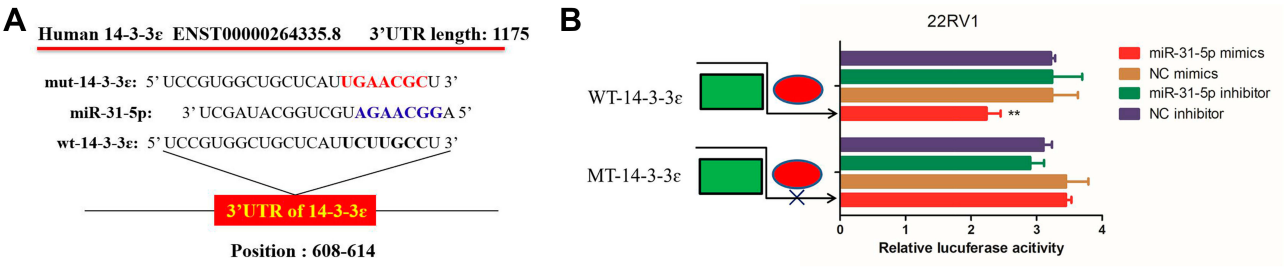

Figure 2 Direct regulation of *14-3-3 ε* by miR-31-5p in 22RV1 cells. (**A**) miR-31-5p binding sites in the 3′-UTR of *14-3-3 ε* mRNA. (**B**) Dual-luciferase reporter assays in 22RV1 using vectors encoding a putative miR-31-5p target site in the *14-3-3 ε* 3′-UTR (positions 608–614). Data were normalized to the expression ratios of Renilla/firefly luciferase activities. miR-31-5p: microRNA-31-5p. $^{**}P<0.01$.
Abbreviations: NC, negative control; WT, wild-type; MUT, mutant.

UALCAN online database was used to analyze the expression of *14-3-3ε* in PRAD (n=497) and normal (n=52) tissues. The results showed that the mRNA expression of *14-3-3ε* was significantly upregulated in PRAD tissues (Figure 3A). To further confirm this result, the protein expression levels of 14-3-3ε were assessed by Western blotting in different PCa cell lines. Figure 3B and C show that the expression of 14-3-3 ε in PC3, LNCaP, and 22RV1 cells was significantly higher than WPMY-1 cells ($P < 0.01$). To investigate the expression of miR-31-5p in PC3, 22RV1, and LNCaP cells, qRT-PCR was used to analyze the expression of miR-31-5p in PCa and normal prostate cells. The results showed that the expression of miR-31-5p was remarkably downregulated in 22RV1 and LNCaP cells ($P < 0.01$). However, no significant difference ($P > 0.05$) in the expression of miR-31-5p was observed between PC3 and WPMY-1 cells (Figure 3D). These results suggest that *14-3-3 ε* acts as a proto-oncogene in PCa, promoting the proliferation of cancer cells. However, miR-31-5p possibly functions as a tumor suppressor factor in 22RV1 and LNCaP cells.

miR-31-5p Overexpression or 14-3-3ε Knockdown Inhibits Proliferation, Invasion, and Migration of 22RV1 Cells

To investigate the role of miR-31-5p and 14-3-3ε in the proliferation, invasion, and migration of 22RV1 cells, the CCK-8 assay and Transwell® assay were performed. miR-31-5p mimics and miR-31-5p inhibitor were used to increase and decrease miR-31-5p expression,

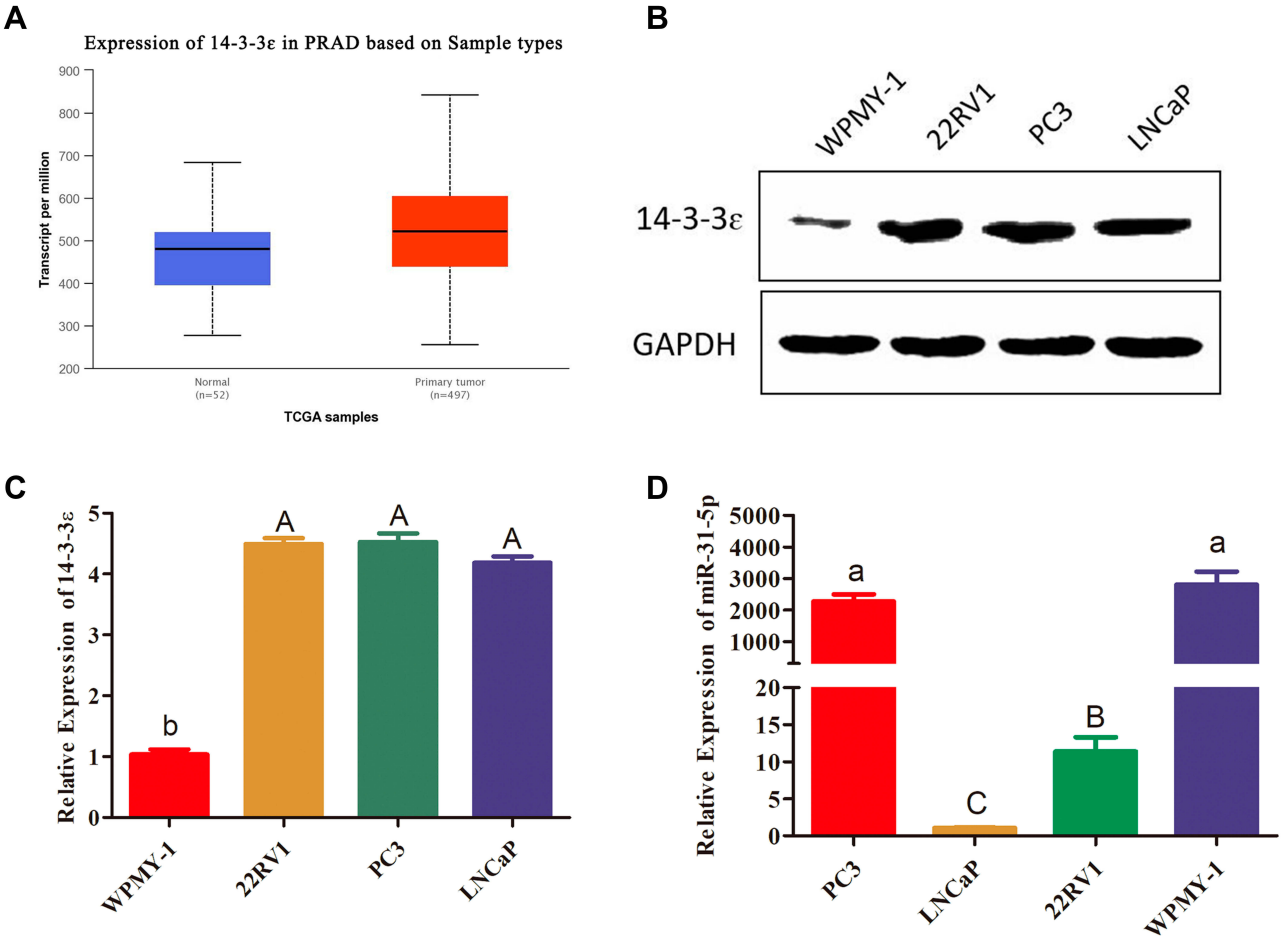

Figure 3 14-3-3 ε and miR-31-5p are differentially expressed in PCa cell lines. (**A**) Compared with 52 normal tissues, the expression level of 14-3-3 ε in 497 PRAD samples significantly increased ($P < 0.01$). These data were quoted from UALCAN-TCGA database. (**B, C**) 14-3-3ε protein expression in PC3, LNCaP, and 22RV1 cells was evaluated by Western blotting. 14-3-3 ε protein expression levels were normalized to GAPDH, and the results are presented as fold changes of expression level. (**D**) miR-31-5p expression in PC3, LNCaP, 22RV1 cells and normal PCa cells (WPMY-1) was evaluated using qRT-PCR. The data in Figure 3B–D are presented as the mean ± SD of values from at least three independent experiments. The values were analyzed by multiple comparative analysis, different capital letters indicate extremely significant differences ($P < 0.01$). Different lowercase letters are significant ($P < 0.05$). The same letter indicates no significant difference ($P > 0.05$).

respectively. miR-31-5p mimics and its corresponding negative control (NC mimics), miR-31-5p inhibitor and its corresponding negative control (NC inhibitor) were transfected into 22RV1 cells. Figure 4A shows that after transfection of 22RV1 cells with miR-31-5p mimics, miR-31-5p expression increased by more than 330-fold compared with those transfected with NC mimic. After transfection with the miR-31-5p inhibitor, the miR-31-5p expression decreased by 68% compared with those transfected with the NC inhibitor. When transfected with the miR-31-5p mimics, 22RV1 cell viability significantly decreased compared to cells transfected with NC mimics ($P < 0.01$) (Figure 4B). After transfection with miR-31-5p inhibitor, 22RV1 cell viability was not significantly different compared to cells transfected with NC inhibitor ($P > 0.05$) (Figure 4B). For cell invasion analysis, the transfection of miR-31-5p mimics in 22RV1 cells reduced cell invasion ($P < 0.01$) compared with the NC mimics. However, the cell invasion ability after transfection of miR-31-5p inhibitor did not significantly differ from those using NC mimics ($P > 0.05$) (Figure 4C). Furthermore, the migration ability of 22RV1 cells significantly decreased in the miR-31-5p mimic group ($P < 0.01$) and significantly increased in the miR-31-5p inhibitor group ($P < 0.05$) (Figure 4D). These results suggest that overexpression of miR-31-5p inhibits the proliferation, invasion, and migration of 22RV1 cells.

According to our analysis in Figure 1, we found that *14-3-3ε* expression was positively correlated with PCa cells. Therefore, to investigate the role of *14-3-3ε* in PCa cells, we downregulated the expression of *14-3-3ε* in 22RV1 cells by transfecting four different double-stranded siRNAs targeting *14-3-3ε* (siRNA-1, siRNA-2, siRNA-3, and siRNA-4). Figure 5A shows that after transfecting the four siRNAs, the siRNA-4 group showed the best inhibitory effect, and 14-3-3ε expression decreased by 96.8% compared with the negative control (siRNA-NC) ($P < 0.01$). In addition, transfecting siRNA-4 significantly decreased cell viability compared with siRNA-NC ($P < 0.01$) (Figure 5B). Cell invasion and migration analyses showed that 14-3-3ε downregulation in 22RV1 cells due to the transfection of siRNA-4 significantly inhibits cell invasion ($P < 0.01$; Figure 5C) and cell migration ($P < 0.01$; Figure 5D). These results suggest that 14-3-3ε downregulation inhibits proliferation, invasion, and migration of 22RV1 cells.

Upregulation of miR-31-5p Suppresses Proliferation, Invasion, and Migration and Promotes Cell Apoptosis of 22RV1 Cells by Inhibiting 14-3-3ε

As demonstrated above, *14-3-3ε* downregulation suppressed proliferation, invasion, and migration of 22RV1 cells. Then, we further confirmed that miR-31-5p directly targets the 3′UTR of *14-3-3ε* to inhibit its expression. Therefore, we hypothesized that miR-31-5p suppresses the proliferation, invasion, and migration and promotes cell apoptosis of 22RV1 cells by inhibiting *14-3-3 ε*. To confirm this hypothesis, a compensation experiment was performed. First, we detected the transfection efficiency of miR-31-5p mimics, NC mimics, miR-31-5p inhibitor, NC inhibitor, pCI-14-3-3ε, and pCI-neo, which were detected by Western blotting at 36 hpt. The results showed that 14-3-3ε expression was downregulated by 4.1-fold after miR-31-5p mimic transfection (Figure 6A), whereas after transfecting pCI-14-3-3ε, 14-3-3ε expression was upregulated by 2.5-fold (Figure 6B). The 22RV1 cells were co-transfected with miR-31-5p mimics + pCI-YWHAE, miR-31-5p mimics + pCI-neo, NC mimics + pCI-YWHAE, and NC mimics and pCI-neo. Figure 6C shows that cell viability was significantly upregulated by *14-3-3ε* knockdown ($P < 0.05$) and downregulated by miR-31-5p upregulation ($P < 0.01$). However, the inhibitory effect of miR-31-5p on cell viability could be partially reversed by *14-3-3ε*. In addition, similar results were observed in the Transwell® (Figure 6D) and scratch wound healing (Figure 6E) assays. The invasion and migration capability of 22RV1 cells were enhanced by *14-3-3ε* and inhibited by miR-31-5p. The inhibitory effect of miR-31-5p on 22RV1 cell invasion and migration was partially reversed by *14-3-3ε*.

Next, we analyzed the effects of miR-31-5p,*14-3-3ε*, and miR-31-5p+*14-3-3ε* on cell apoptosis of 22RV1 (Figure 7A). The results showed that the ratios of cell apoptosis and cell necrosis in the miR-31-5p group were extremely significantly increased ($P < 0.01$) compared with the other groups. However, the opposite result was observed in the pCI-14-3-3 ε group. Interestingly, when miR-31-5p mimics and pCI-14-3-3ε were co-transfected into 22RV1 cells, the pro-apoptotic effect of miR-31-5p was partially reversed by *14-3-3ε* (Figure 7B and C). These results indicate that miR-31-5p suppresses PCa proliferation, invasion, and migration and promotes 22RV1 cell apoptosis by inhibiting *14-3-3 ε*.

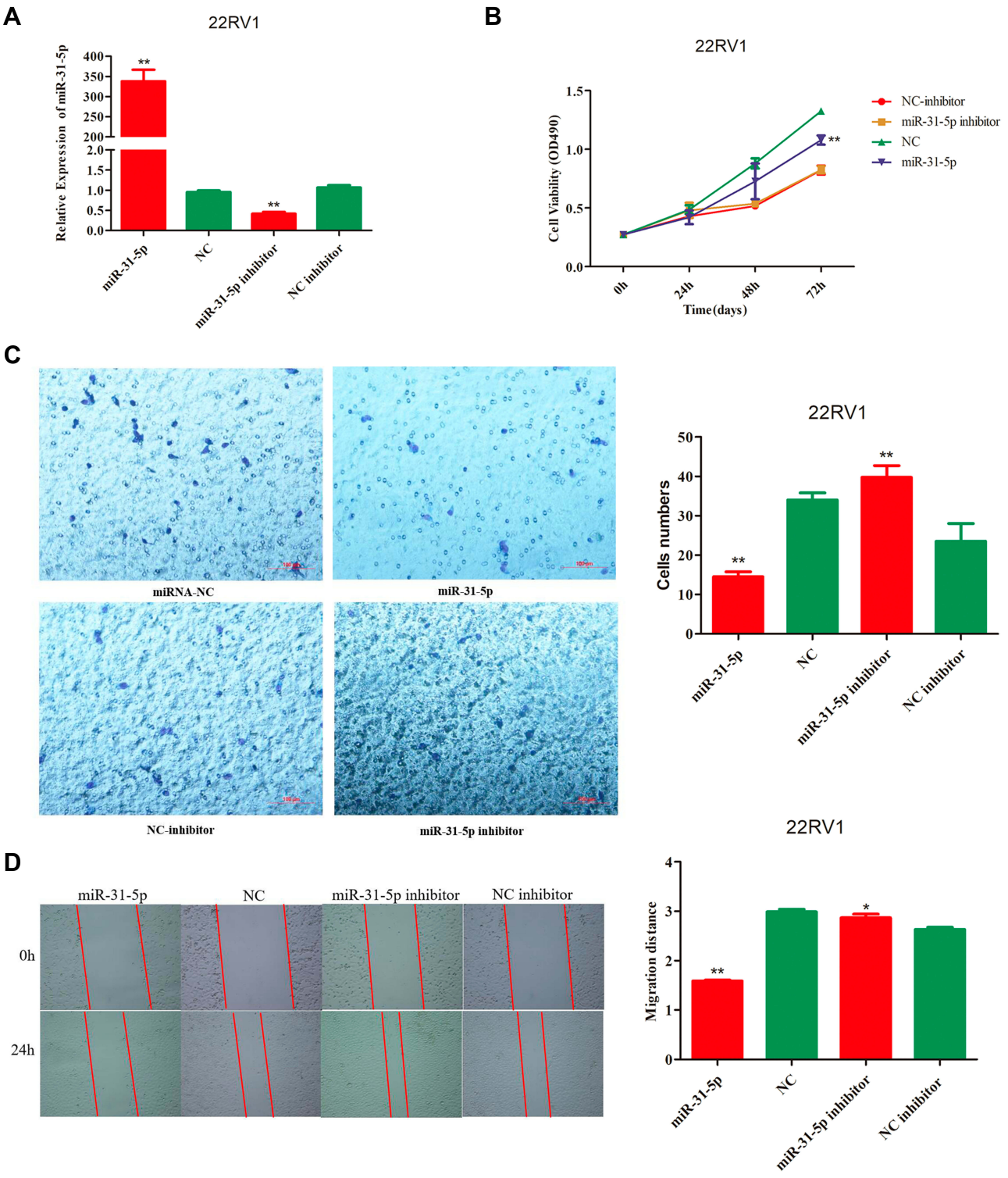

Figure 4 The overexpression of miR-31-5p inhibits the proliferation, invasion, and migration of 22RV1 cells. (**A**) The transfection efficiency of miR-31-5p mimics and miR-31-5p inhibitor in 22RV1 cell lines were assessed by qRT-PCR at 24 hours post transfection (hpt). (**B**) The effects of overexpression and inhibition of miR-31-5p expression on the proliferation of 22RV1 cells. The CCK-8 assay showed that the overexpression of miR-31-5p significantly inhibits cell proliferation compared with the NC mimics at 72 hpt ($P<0.01$). (**C**) The effects of overexpression and inhibition of miR-31-5p expression on the invasion of 22RV1 cells. The Transwell® assay showed that the overexpression of miR-31-5p significantly inhibits cell migration compared with the NC mimics ($P<0.01$). The proliferation and migration abilities of the miR-31-5p inhibitor and NC inhibitor groups did not significantly differ ($P>0.05$). (**D**) Representative images of migration assays using 22RV1 cells. Magnification, 100×. Quantification of relative migration of 22RV1 cells transfected with miR-31-5p mimic, NC mimic, miR-31-5p inhibitor, or NC inhibitor. The data in the figure are presented as the mean ± standard deviation of three independent experiments. Statistical significance was determined using the Student's *t*-test. *$P < 0.05$, **$P < 0.01$ vs control group.

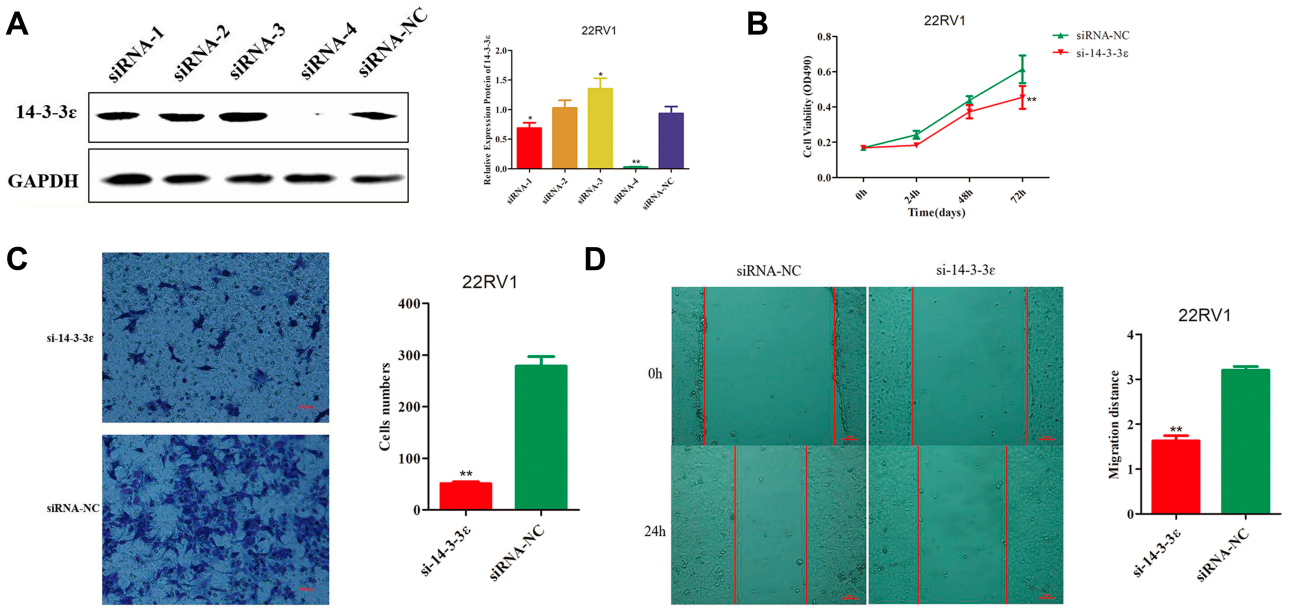

Figure 5 Effect of 14-3-3 ε silencing in 22RV1 cells. (**A**) 14-3-3 ε protein expression was evaluated by Western blotting analysis of 22RV1 cells 48 h post transfection (hpt) with siRNA-1, siRNA-2, siRNA-3, and siRNA-4. GAPDH was used as internal control. (**B**) Cell viability was determined using CCK-8 assays at 0, 24, 48, and 72 hpt, analysis of 22RV1cells 48 hpt with si-14-3-3 ε(*siRNA*-4). siRNA-NC was used as negative control. (**C**) Cell invasion potency of 22RV1 cells was evaluated using the Transwell® assay following transfection with si-14-3-3 ε and siRNA-NC. Five fields from each chamber were photographed and counted. (**D**) Cell migration potency in 22RV1 cells was evaluated using scratch wound healing assays following transfection with si-14-3-3 ε and siRNA-NC. Magnification, 100×. Statistical significance was determined using the Student's *t*-test. $^{*}P < 0.05$, $^{**}P < 0.01$.

Previous studies have illustrated that the PI3K/Akt pathway plays an important role in regulating the proliferation of PCa cells, and the ratios of p-PI3K/PI3K and p-AKT/AKT were positively correlated to the proliferation of cancer cells.[30,31] Therefore, to explore the effects of miR-31-5p that targets 14-3-3ε on the PI3K/Akt pathway, 22RV1 cells were divided into five groups and transfected with miR-31-5p mimics, NC mimics, pCI-14-3-3ε, pCI-neo, and miR-31-5p mimics + pCI-14-3-3ε. By analyzing the expression levels of p-PI3K/PI3K and p-AKT/AKT, we elucidated the relationship of miR-31-5p, 14-3-3ε, and the PI3K/AKT signaling pathway. The results showed that the p-PI3K/PI3K and p-AKT/AKT ratios followed a similar trend, which were significantly downregulated in the transfected miR-31-5p group compared with the transfected NC group ($P < 0.01$) and were significantly up-regulated in the pCI-14-3-3ε group compared with the transfected pCI-neo group ($P < 0.01$). When co-transfected with miR-31-5p+14-3-3ε, the ratio of p-PI3K/PI3K and p-AKT/AKT increased, indicating that the compensation of *14-3-3ε* partially reversed the regulatory effect of miR-31-5p on the proliferation of PCa cells (Figure 8A–C). These results suggest that p-PI3K, PI3K, p-AKT, and AKT proteins may be directly involved in the effect of miR-31-5p targeted regulation of *14-3-3ε* on the proliferation of 22RV-1 PCa cells.

In addition, studies have shown that 14-3-3 proteins regulate apoptosis; these inhibit apoptosis through interactions with members of the Bcl-2 family and by regulating apoptosis-related signaling pathways or transcription factors. Therefore, we hypothesize that miR-31-5p regulates *14-3-3ε* through the same mechanism by which it promotes cell apoptosis. It has been proposed that high Bax and/or low Bcl-2 expression levels as well as high Bax/Bcl-2 ratio favor apoptosis.[32,33] In addition, the increase in BAD expression and the activation of the caspase pathway are also important indicators of apoptosis. Here, key proteins such as BAD, 14-3-3ε, BAX/Bcl-2, pro-caspase 9, and full-length caspase 3 were detected by Western blotting (Figure 9A). The results show that 14-3-3ε and BAD exhibit opposite expression patterns (Figure 9B), whereas pro-caspase 9 and full-length caspase-3 depict similar expression patterns (Figure 9C). The expression levels of 14-3-3ε, pro-caspase-9 and full-length caspase-3 in the miR-31-5p mimic group significantly decreased compared to the other groups ($P < 0.05$), whereas the BAD expression and Bax/Bcl-2 ratios markedly increased ($P < 0.01$) (Figure 9B). However, the opposite trend was observed in the pCI-14-3-3 ε group. Then, we co-transfected miR-31-5p mimics and pCI-14-3-3ε into 22RV1 cells, which showed that the pro-apoptotic effect of miR-31-5p was

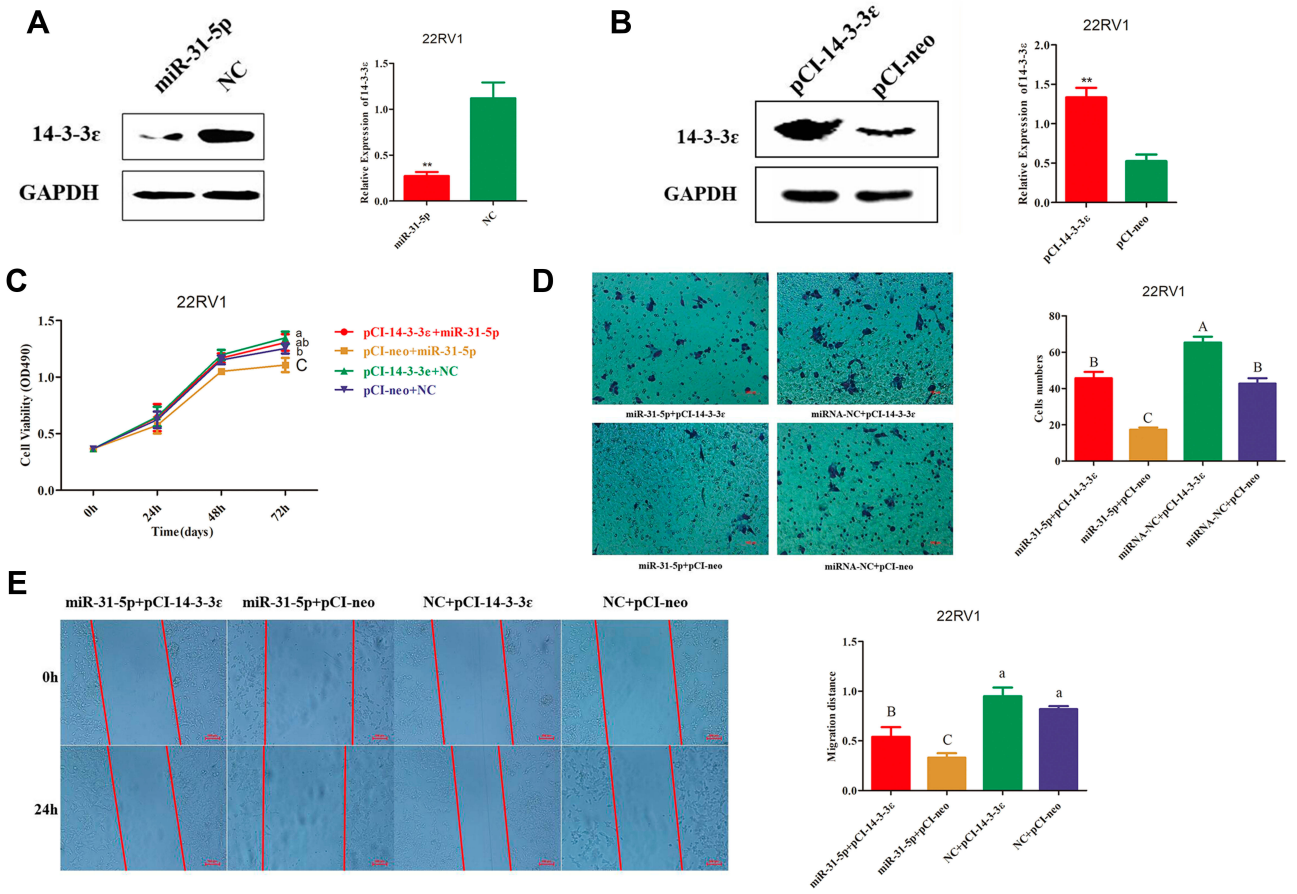

Figure 6 Effects of *14-3-3ε/miR-31-5p* co-transfection on 22RV1 cells. (**A, B**) Transfection efficiency using miR-31-5p mimics, NC mimics, pCI-14-3-3 ε, and pCI-neo into 22RV1 cells was evaluated by Western blotting assay at 48 h post transfection. (**C**) CCK-8 assay revealed the inhibitory effect of miR-31-5p on 22RV1 cell viability after upregulation of 14-3-3ε expression. (**D**) Transwell® assay indicated the inhibitory effect of miR-31-5p on 22RV1 cell invasion after upregulation of 14-3-3ε expression. (**E**) Scratch wound healing assays exhibited the inhibitory effect of miR-31-5p on 22RV1 cell migration after upregulation of 14-3-3ε expression. Statistical significance was determined using the Student's *t*-test (**A** and (**B**). $^{**}P < 0.01$. Statistical significance was determined using multiple comparative analysis (**C**–**E**), different capital letters indicate extremely significant differences ($P < 0.01$). Different lowercase letters indicate significant differences ($P < 0.05$). The same letter indicates no significant difference ($P > 0.05$).

partially reversed by 14-3-3ε (Figure 9A–D). These results imply that miR-31-5p inhibits cell proliferation and promotes cell apoptosis in 22RV1 by regulating *14-3-3ε* via the PI3K/AKT/Bcl-2 signaling pathway.

Discussion

CRPC is a type of PCa in which the disease progresses after initial sustained ADT. Androgen deprivation is the mainstay of advanced prostate cancer treatment. Despite initial responses, almost all patients progress to CRPC.[34] Treatment of patients with mCRPC remains a significant clinical challenge.[35] AR plays an important role in the treatment of mCRPC.[6] Recently, one study reported that members of the 14-3-3 family play an important role in the development and progression of PCa by regulating the transcription of PSA through the AR.[8] 14-3-3ε belongs to the 14-3-3 family, which was first identified in mammalian brain tissues by Moor and Perez in 1968.[36] Previous studies have implicated 14-3-3ε as a cell enhancer factor that promotes cell proliferation in breast cancer cells,[12] gastric cancer SGC7901 cells,[37] and hepatocellular carcinoma[14] and as a potential novel genetic risk factor for HIV neurocognitive impairment,[24] major depressive disorder in males of the Chinese Han population,[38] and development of midline craniofacial structures.[39] Recently, Alex and colleagues[9] suggested that 14-3-3ε and other family members play an important role in the development and progression of PCa, indicating that it can be employed as a drug target in the treatment of PCa. In the present study, we found that 14-3-3ε is significantly upregulated in PCa cell lines and acts as a cell enhancer factor to promote PCa cell proliferation, migration, and invasion. Therefore, we hypothesized that 14-3-3ε acts as a proto-oncogene in PCa, promoting the proliferation of cancer cells. miRNAs have a large regulatory potential and

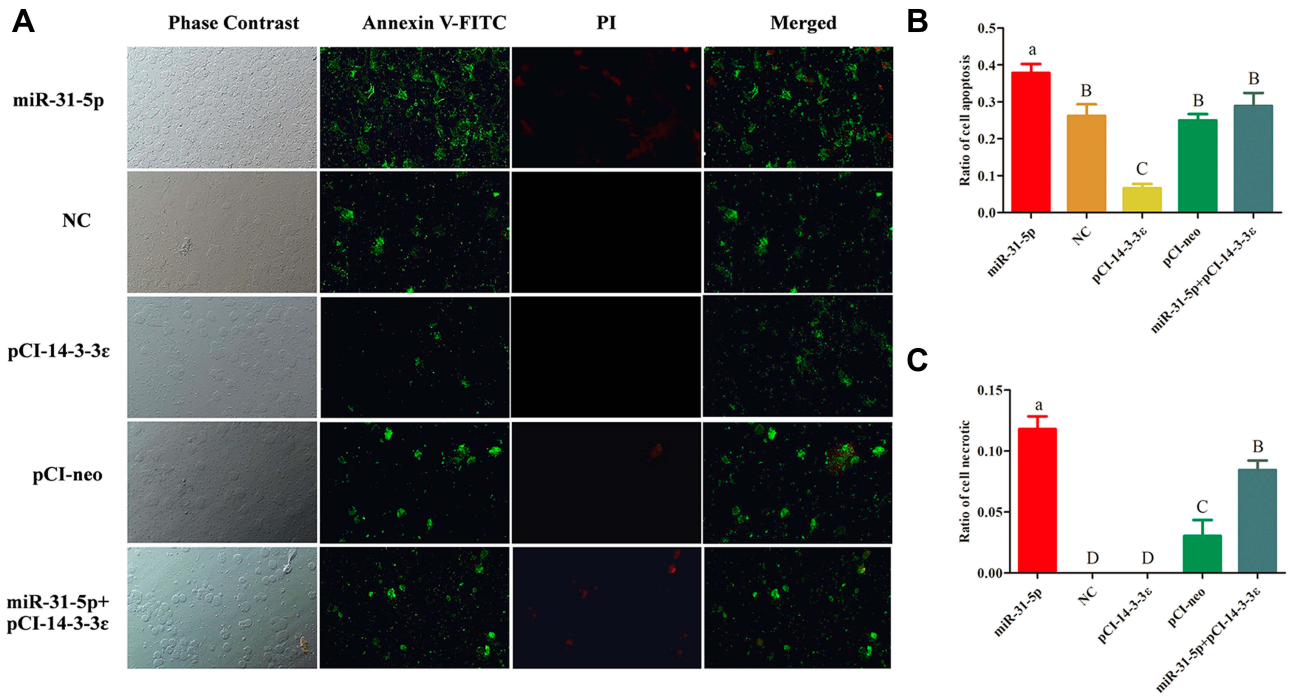

Figure 7 Annexin V-FITC and propidium iodide (PI) staining. (**A**) Morphological changes in 22RV-I cells were detected using fluorescence microscopy. Only the apoptotic cells showed green fluorescence, necrotic cells exhibited both green and red fluorescence, and normal cells did not depict any fluorescence. (**B, C**) The apoptotic and necrotic rates of each treatment were assessed. Statistical significance was determined using multiple comparative analysis (**A–C**); different capital letters indicate extremely significant differences ($P < 0.01$). Different lowercase letters indicate significant differences ($P < 0.05$). The same letter indicates no significant difference ($P > 0.05$).

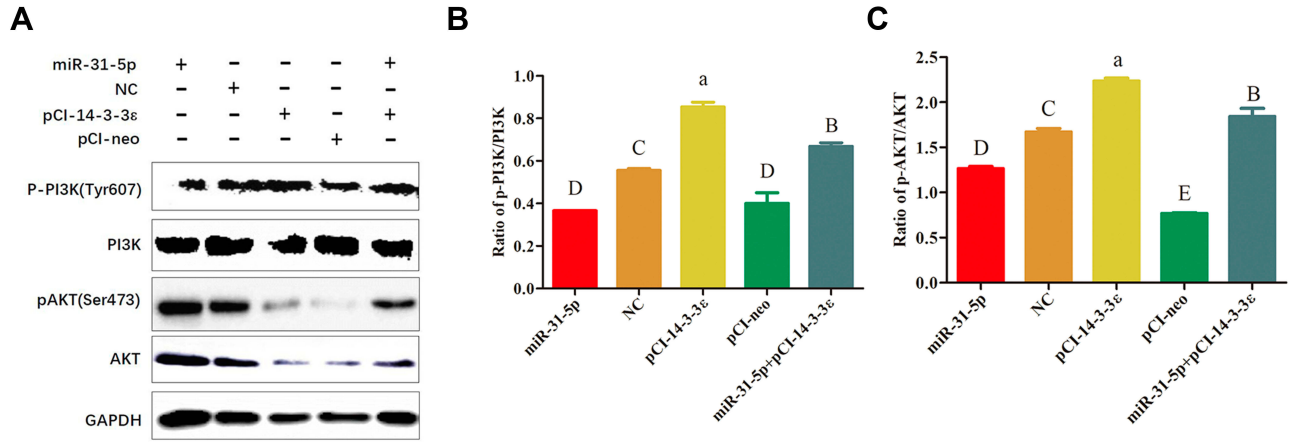

Figure 8 The effect of miR-31-5p on the ratio of p-PI3K/PI3K and p-AKT/AKT in regulating 14-3-3ε expression. (**A**) Western blot analysis was performed to evaluate the expression of p-PI3K, PI3K, p-AKT, and AKT in 22RV1 cells treated with miR-31-5p, negative control, pCI-14-3-3 ε, pCI-neo, and miR-31-5p+pCI-14-3-3ε. (**B**) Effects of different treatment groups on p-PI3K/PI3K protein expression. (**C**) Effects of different treatment groups on p-AKT/AKT protein expression. Statistical significance was determined using multiple comparative analysis; different capital letters indicate extremely significant differences ($P < 0.01$). Different lowercase letters represent significant differences ($P < 0.05$). The same letter indicates no significant difference ($P > 0.05$).

are estimated to regulate 30% of genes in the human genome.[40] Consequently, finding miRNAs that are negatively correlated with *14-3-3ε* expression and regulate their expression may be another way to diagnose and treat PCa.

In the present study, we found that *14-3-3ε* exhibits the opposite expression pattern with miR-31-5p in PCa cells. Moreover, among the 5 candidate miRNAs that regulate *14-3-3ε*, miR-31-5p showed superior inhibitory efficiency. A previous study indicated that miR-31-5p is differentially expressed in various kinds of cancers, and whether miR-31-5p acts as an inducer or inhibitor of tumors varies with tumor types.[41] Peng et al reported that miR-31-5p is

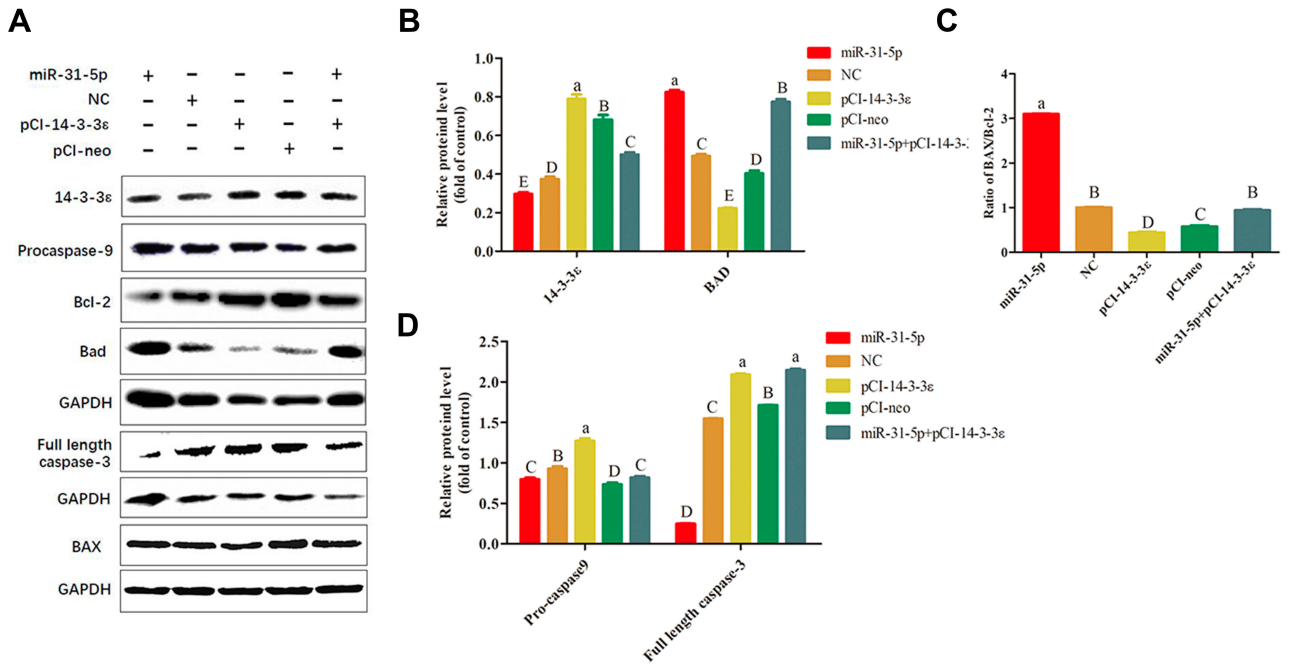

Figure 9 miR-31-5p regulates 14-3-3ε-induced apoptosis in 22RV1 cells via the Bcl-2 pathway. (**A**) Western blot analysis of key proteins related to Bcl-2 apoptosis pathway in 22RV1 cells transfected with miR-31-5p, negative control, pCI-14-3-3ε, pCI-neo, and miR-31-5p+pCI-14-3-3ε. (**B**) Western blot analysis of 14-3-3ε and BAD in 22RV1cells. (**C**) Western blot analysis of BAX/Bcl2 ratios in 22RV1 cells. (**D**) Western blot analysis of pro-caspase-9 and full-length caspase-3 in 22RV1 cells. Statistical significance was determined using multiple comparative analysis; different capital letters indicate extremely significant differences ($P < 0.01$). Different lowercase letters reveal significant differences ($P < 0.05$). The same letter indicates no significant difference ($P > 0.05$).

upregulated in colorectal cancer and functions as a tumor promoter by targeting NUMB.[25] Furthermore, miR-31-5p also acts as a tumor promoter in osteosarcoma via the Wnt/β-catenin signaling pathway by enhancing AXIN1 expression.[42] Furthermore, Zhao et al reported that miR-31-5p acts as a tumor suppressor in HepG2 hepatocellular carcinoma cell by regulating the expression of Sp1 transcription factor.[41] Li found that miR-31-5p also acts as a tumor suppressor in renal cell carcinoma by targeting CDK1.[43] The results of our study indicate that the expression of miR-31-5p in PCa is similar to that in hepatocellular carcinoma and renal cell carcinoma, thereby suggesting that it acts as a tumor suppressor by regulating *14-3-3ε* expression.

An earlier investigation suggested that the key role of 14-3-3 proteins involves balancing the AR and PI3K-AKT-mTOR protein network.[44] PI3K/AKT is a set of vital kinases that play a pivotal role in the regulation of genes associated with apoptosis.[45] The activation of the PI3K/AKT signaling pathway results in the regulation of proliferation of PCa cells, and the ratios of p-PI3K/PI3K and p-AKT/AKT were positively correlated to cell proliferation and cell apoptosis.[30,31] In addition, PI3K/Akt is intimately related to Bcl-2 family proteins, which are crucial apoptosis-associated factors of mitochondria.[45] More studies have found that members of the Bcl-2 protein family play an important role in 14-3-3-mediated cell proliferation and apoptosis.[46–48] As one of the pro-apoptotic proteins of the Bcl-2 family, BAD is phosphorylated by Akt, and 14-3-3 then binds to the phosphorylated BAD to induce conformational changes in BAD and promote the separation of BAD from Bcl-2/Bcl-XL, thereby blocking the precursor effect of BAD apoptosis.[49–51] Furthermore, the 14-3-3 protein can bind to the apoptosis-regulating protein BAX of the Bcl-2 family, which prevents BAX from entering the mitochondria and thus terminating the regulatory effect of BAX on apoptosis.[52–56] It has been proposed that high p-PI3K/PI3K and p-AKT/AKT ratios favor cell proliferation[30,31] and high BAX and/or low Bcl-2 as well as high BAX/Bcl-2 ratio favor apoptosis.[32,33]

Therefore, to investigate the effects of miR-31-5p regulation of *14-3-3ε* on the PI3K/AKT signaling pathway and the Bcl-2 family, p-PI3K/PI3K, p-AKT/AKT BAD, 14-3-3 ε, BAX/Bcl-2, pro-caspase-9, and full-length caspase-3 were detected by Western blotting. Our results indicate that the p-PI3K/PI3K and p-AKT/AKT ratios showed opposite results in the miR-31-5p and 14-3-3ε transfection groups, and the complementary experiment

partially reversed the effects on the ratios of p-PI3K/PI3K and p-AKT/AKT. The expression levels of 14-3-3ε, pro-caspase-9, and full-length caspase-3 markedly decreased in the miR-31-5p transfection group, whereas those of BAD and BAX/Bcl-2 significantly increased. However, the opposite result was observed in the 14-3-3 ε group. Similarly, the complementary experiment partially reversed the expression levels of these proteins (Figure 9A–D). These results imply that miR-31-5p acts as a tumor suppressor in 22RV1 cells and inhibits cell survival and proliferation by regulating *14-3-3ε* expression via the PI3K/AKT/Bcl-2 signaling pathway.

Conclusions

miR-31-5p acts as a tumor suppressor in 22RV1 cells and inhibits cell survival and proliferation by regulating *14-3-3ε* expression and survival- and proliferation-related signaling pathways. These results provide a theoretical basis for further investigating whether miR-31-5p and *14-3-3ε* act as potential prognostic biomarkers and may potentially be utilized as therapeutic targets for PCa treatment.

Acknowledgments

This work was supported by the Scientific Research Cooperation Project with America and Oceania Region, Ministry of Education (Grant No. JCSH[2017]860), Natural Science Foundation of China (Grant No. 31860242), Guizhou Province Science and Technology Plan Project (Grant No. Guizhou Branch Platform Talents [2017]5788), and Key Laboratory of Animal Genetics, Breeding, and Reproduction in The Plateau Mountainous Region, Ministry of Education, Guizhou University (Grant No. GYSD-K-2018-06). We thank LetPub for its linguistic assistance during the preparation of this manuscript.

Disclosure

All authors have no competing interests to declare.

References

1. Du LB, Li HZ, Wang XH, et al. Analysis of cancer incidence in Zhejiang cancer registry in China during 2000 to 2009. *Asian Pac J Cancer Prev*. 2014;15(14):5839–5843. doi:10.7314/APJCP.2014.15.14.5839
2. Wu M, Huang Y, Chen T, et al. LncRNA MEG3 inhibits the progression of prostate cancer by modulating miR-9-5p/QKI-5 axis. *J Cell Mol Med*. 2019;23(1):29–38. doi:10.1111/jcmm.13658
3. National cancer institute. Prostate cancer treatment. 2018:https://www.cancer.gov/types/prostate/hp/prostate-treatment-pdq. Accessed July 9, 2020.
4. Taghizadeh H, Marhold M, Tomasich E, Udovica S, Merchant A, Krainer M. Immune checkpoint inhibitors in mCRPC - rationales, challenges and perspectives. *Oncoimmunology*. 2019;8(11):e1644109. doi:10.1080/2162402X.2019.1644109
5. Feldman BJ, Feldman D. The development of androgen-independent prostate cancer. *Nat Rev Cancer*. 2001;1(1):34–45. doi:10.1038/35094009
6. Gillessen SOAAG. Management of patients with advanced prostate cancer: recommendations of the St gallen advanced prostate cancer consensus conference (APCCC) 2015. *Ann Oncol*. 2019;30(12):e3. doi:10.1093/annonc/mdw180
7. Rebecca L, Siegel KDMA. Cancer statistics, 2018. *CA Cancer J Clin*. 2018;68:7–30.
8. Quayle SN, Sadar MD. 14-3-3 sigma increases the transcriptional activity of the androgen receptor in the absence of androgens. *Cancer Lett*. 2007;254:137–145.
9. Root A, Beizaei A, Ebhardt HA. Structure-based assessment and network analysis of targeting 14-3-3 proteins in prostate cancer. *Mol Cancer*. 2018;17:156.
10. Zhao R, He H, Zhu Y, et al. MiR-204/14-3-3zeta axis regulates osteosarcoma cell proliferation through SATA3 pathway. *Pharmazie*. 2017;72(10):593–598. doi:10.1692/ph.2017.7574
11. Aghazadeh Y, Papadopoulos V. The role of the 14-3-3 protein family in health, disease, and drug development. *Drug Discov Today*. 2016;21(2):278–287. doi:10.1016/j.drudis.2015.09.012
12. Yang YF, Lee YC, Wang YY, Wang CH, Hou MF, Yuan SF. YWHAE promotes proliferation, metastasis, and chemoresistance in breast cancer cells. *Kaohsiung J Med Sci*. 2019;35(7):408–416. doi:10.1002/kjm2.12075
13. Luk SC, Garcia-Barcelo M, Tsui SK, Fung KP, Lee CY, Waye MM. Assignment of the human 14-3-3 epsilon isoform (YWHAE) to human chromosome 17p13 by in situ hybridization. *Cytogenet Cell Genet*. 1997;78(2):105–106. doi:10.1159/000134638
14. Liu T, Jan Y, Ko B, et al. 14-3-3ε overexpression contributes to epithelial-mesenchymal transition of hepatocellular carcinoma. *PLoS One*. 2013;8(3):e57968. doi:10.1371/journal.pone.0057968
15. Qi W, Liu X, Qiao D, Martinez JD. Isoform-specific expression of 14-3-3 proteins in human lung cancer tissues. *Int J Cancer*. 2005;113(3):359–363. doi:10.1002/ijc.20492
16. Li DQ, Wang L, Fei F, et al. Identification of breast cancer metastasis-associated proteins in an isogenic tumor metastasis model using two-dimensional gel electrophoresis and liquid chromatography-ion trap-mass spectrometry. *Proteomics*. 2006;6(11):3352–3368. doi:10.1002/pmic.200500617
17. Wang Z, Nesland JM, Suo Z, Trope CG, Holm R. The prognostic value of 14-3-3 isoforms in vulvar squamous cell carcinoma cases: 14-3-3beta and epsilon are independent prognostic factors for these tumors. *PLoS One*. 2011;6(9):e24843. doi:10.1371/journal.pone.0024843
18. Sofiadis A, Becker S, Hellman U, et al. Proteomic profiling of follicular and papillary thyroid tumors. *Eur J Endocrinol*. 2012;166(4):657–667. doi:10.1530/EJE-11-0856
19. Liu Y, Tian R, Li Y, et al. The expression of seven 14-3-3 isoforms in human meningioma. *Brain Res*. 2010;1336:98–102. doi:10.1016/j.brainres.2010.04.009
20. Ko BS, Chang TC, Hsu C, et al. Overexpression of 14-3-3epsilon predicts tumour metastasis and poor survival in hepatocellular carcinoma. *Histopathology*. 2011;58(5):705–711. doi:10.1111/j.1365-2559.2011.03789.x
21. Mariana FLDQ. Clinical implication of 14-3-3 epsilon expression in gastric cancer. *World J Gastroenterol*. 2012;18(13):1531–1537. doi:10.3748/wjg.v18.i13.1531
22. Liou J, Ghelani D, Yeh S, Wu KK. Nonsteroidal Anti-inflammatory Drugs induce colorectal cancer cell apoptosis by suppressing 14-3-3ε. *Cancer Res*. 2007;67(7):3185–3191. doi:10.1158/0008-5472.CAN-06-3431

23. Liang S, Xu Y, Shen G, et al. Quantitative protein expression profiling of 14-3-3 isoforms in human renal carcinoma shows 14-3-3 epsilon is involved in limitedly increasing renal cell proliferation. *Electrophoresis*. 2009;30(23):4152–4162. doi:10.1002/elps.200900249
24. Morales D, Hechavarria R, Wojna V, Acevedo SF. YWHAE/14-3-3epsilon: a potential novel genetic risk factor and CSF biomarker for HIV neurocognitive impairment. *J Neurovirol*. 2013;19(5):471–478. doi:10.1007/s13365-013-0200-z
25. Peng H, Wang L, Su Q, Yi K, Du J, Wang Z. MiR-31-5p promotes the cell growth, migration and invasion of colorectal cancer cells by targeting NUMB. *Biomed Pharmacother*. 2019;109:208–216. doi:10.1016/j.biopha.2018.10.048
26. Filella X, Foj L. miRNAs as novel biomarkers in the management of prostate cancer. *Clin Chem Lab Med*. 2017;55(5):715–736. doi:10.1515/cclm-2015-1073
27. Song S, Sun K, Dong J, et al. microRNA-29a regulates liver tumor-initiating cells expansion via Bcl-2 pathway. *Exp Cell Res*. 2020;387(2):111781. doi:10.1016/j.yexcr.2019.111781
28. van Bokhoven A, Varella-Garcia M, Korch C, et al. Molecular characterization of human prostate carcinoma cell lines. *Prostate*. 2003;57(3):205–225. doi:10.1002/pros.10290
29. Sramkoski RM, Pretlow TN, Giaconia JM, et al. A new human prostate carcinoma cell line, 22Rv1. *In Vitro Cell Dev Biol Anim*. 1999;35(7):403–409. doi:10.1007/s11626-999-0115-4
30. Wang Z, Wang Y, Zhu S, et al. DT-13 inhibits proliferation and metastasis of human prostate cancer cells through blocking PI3K/Akt Pathway. *Front Pharmacol*. 2018;9:1450. doi:10.3389/fphar.2018.01450
31. Sachan R, Kundu A, Jeon Y, et al. Afrocyclamin A, a triterpene saponin, induces apoptosis and autophagic cell death via the PI3K/Akt/mTOR pathway in human prostate cancer cells. *Phytomedicine*. 2018;51:139–150. doi:10.1016/j.phymed.2018.10.012
32. Singh L, Pushker N, Saini N, et al. Expression of pro-apoptotic Bax and anti-apoptotic Bcl-2 proteins in human retinoblastoma. *Clin Exp Ophthalmol*. 2015;43(3):259–267. doi:10.1111/ceo.12397
33. Kulsoom B, Shamsi TS, Afsar NA, Memon Z, Ahmed N, Hasnain SN. Bax, Bcl-2, and Bax/Bcl-2 as prognostic markers in acute myeloid leukemia: are we ready for Bcl-2-directed therapy? *Cancer Manag Res*. 2018;10:403–416. doi:10.2147/CMAR.S154608
34. Tucci M, Scagliotti GV, Vignani F. Metastatic castration-resistant prostate cancer: time for innovation. *Future Oncol*. 2015;11(1):91–106. doi:10.2217/fon.14.145
35. Sartor AO. Progression of metastatic castrate-resistant prostate cancer: impact of therapeutic intervention in the post-docetaxel space. *J Hematol Oncol*. 2011;4(1):18. doi:10.1186/1756-8722-4-18
36. Moore BW, Perez VJ, Gehring M. Assay and regional distribution of a soluble protein characteristic of the nervous system. *J Neurochem*. 1968;15(4):265–272. doi:10.1111/j.1471-4159.1968.tb11610.x
37. Yan L, Gu H, Li J, et al. RKIP and 14-3-3epsilon exert an opposite effect on human gastric cancer cells SGC7901 by regulating the ERK/MAPK pathway differently. *Dig Dis Sci*. 2013;58(2):389–396. doi:10.1007/s10620-012-2341-y
38. Liu J, Zhang HX, Li ZQ, et al. The YWHAE gene confers risk to major depressive disorder in the male group of Chinese Han population. *Prog Neuropsychopharmacol Biol Psychiatry*. 2017;77:172–177. doi:10.1016/j.pnpbp.2017.04.013
39. Tucker ME, Escobar LF. Cleft lip/palate associated with 17p13.3 duplication involving a single candidate gene (YWHAE). *Clin Genet*. 2014;85(6):600–601. doi:10.1111/cge.12237
40. Lewis BP, Burge CB, Bartel DP. Conserved seed pairing, often flanked by adenosines, indicates that thousands of human genes are microRNA targets. *Cell*. 2005;120(1):15–20. doi:10.1016/j.cell.2004.12.035
41. Zhao G, Han C, Zhang Z, Wang L, Xu J. Increased expression of microRNA-31-5p inhibits cell proliferation, migration, and invasion via regulating Sp1 transcription factor in HepG2 hepatocellular carcinoma cell line. *Biochem Bioph Res Co*. 2017;490(2):371–377. doi:10.1016/j.bbrc.2017.06.050
42. Chen X, Zhong L, Li X, Liu W, Zhao Y, Li J. Down-regulation of microRNA-31-5p inhibits proliferation and invasion of osteosarcoma cells through Wnt/β-catenin signaling pathway by enhancing AXIN1. *Exp Mol Pathol*. 2019;108:32–41. doi:10.1016/j.yexmp.2019.03.001
43. Li Y, Quan J, Chen F, et al. MiR-31-5p acts as a tumor suppressor in renal cell carcinoma by targeting cyclin-dependent kinase 1 (CDK1). *Biomed Pharmacother*. 2019;111:517–526. doi:10.1016/j.biopha.2018.12.102
44. Ebhardt HA, Root A, Liu Y, Gauthier NP, Sander C, Aebersold R. Systems pharmacology using mass spectrometry identifies critical response nodes in prostate cancer. *NPJ Syst Biol Appl*. 2018;4(1):26. doi:10.1038/s41540-018-0064-1
45. Fu Z, Yang J, Wei Y, Li J. Effects of piceatannol and pterostilbene against beta-amyloid-induced apoptosis on the PI3K/Akt/Bad signaling pathway in PC12 cells. *Food Funct*. 2016;7(2):1014–1023. doi:10.1039/C5FO01124H
46. Mann J, Githaka JM, Buckland TW, et al. Non-canonical BAD activity regulates breast cancer cell and tumor growth via 14-3-3 binding and mitochondrial metabolism. *Oncogene*. 2019;38(18):3325–3339. doi:10.1038/s41388-018-0673-6
47. Tan Y, Demeter MR, Ruan H, Comb MJ. BAD Ser-155 Phosphorylation Regulates BAD/Bcl-XL Interaction and Cell Survival. *J Biol Chem*. 2000;275(33):25865–25869. doi:10.1074/jbc.M004199200
48. He QQ, Wu X, Liu XP, Yang XJ, Yuan ZM, Zhang Y. 14-3-3 epsilon plays an important role in testicular germ cell apoptosis: A functional proteomic study of experimental varicocele. *Andrologia*. 2019;51(6):e13275. doi:10.1111/and.13275
49. Datta SR, Katsov A, Hu L, et al. 14-3-3 proteins and survival kinases cooperate to inactivate BAD by BH3 domain phosphorylation. *Mol Cell*. 2000;6(1):41–51. doi:10.1016/S1097-2765(05)00012-2
50. Patel MP, Masood A, Patel PS, Chanan-Khan AA. Targeting the Bcl-2. *Curr Opin Oncol*. 2009;21(6):516–523. doi:10.1097/CCO.0b013e328331a7a4
51. She Q, Solit DB, Ye Q, O Reilly KE, Lobo J, Rosen N. The BAD protein integrates survival signaling by EGFR/MAPK and PI3K/Akt kinase pathways in PTEN-deficient tumor cells. *Cancer Cell*. 2005;8(4):287–297. doi:10.1016/j.ccr.2005.09.006
52. Nomura M, Shimizu S, Sugiyama T, et al. 14-3-3 interacts directly with and negatively regulates pro-apoptotic Bax. *J Biol Chem*. 2015;290(11):6753. doi:10.1074/jbc.A114.207880
53. Tang Y, Lv P, Sun Z, Han L, Luo B, Zhou W. 14-3-3zeta up-regulates hypoxia-inducible factor-1alpha in hepatocellular carcinoma via activation of PI3K/Akt/NF-small ka, CyrillicB signal transduction pathway. *Int J Clin Exp Pathol*. 2015;8(12):15845–15853.
54. Zeng K, Wang X, Ko H, Kwon HC, Cha JW, Yang HO. Hyperoside protects primary rat cortical neurons from neurotoxicity induced by amyloid β-protein via the PI3K/Akt/Bad/BclXL-regulated mitochondrial apoptotic pathway. *Eur J Pharmacol*. 2011;672(1–3):45–55. doi:10.1016/j.ejphar.2011.09.177
55. Min S, Liang X, Zhang M, et al. Multiple Tumor-Associated MicroRNAs Modulate the Survival and Longevity of Dendritic Cells by Targeting YWHAZ and Bcl2 Signaling Pathways. *J Immunol*. 2013;190(5):2437–2446. doi:10.4049/jimmunol.1202282
56. Liu D, Yi B, Liao Z, et al. 14-3-3gamma protein attenuates lipopolysaccharide-induced cardiomyocytes injury through the Bcl-2 family/mitochondria pathway. *Int Immunopharmacol*. 2014;21(2):509–515. doi:10.1016/j.intimp.2014.06.014